Journal of Modern Optics
Vol. 54, No. 11, 20 July 2007, 1619–1626

Transfer of trapped atoms between two optical tweezer potentials

M. SCHULZ†‡, H. CREPAZ†§, F. SCHMIDT-KALER†¶,
J. ESCHNER*†§ and R. BLATT†

†Institut für Experimentalphysik, Universität Innsbruck, Austria

(*Received 23 May 2006*)

Trapped, laser-cooled rubidium atoms are transferred between two strongly focused, horizontal, orthogonally intersecting laser beams. The transfer efficiency is studied as a function of the vertical distance between the beam axes. Optimum transfer is found when the distance equals the beam waist radius. Numerical simulations reproduce well the experimental results.

1. Introduction

The spatial control of atoms, beyond their trapping in stationary potentials, has been continuously gaining importance in investigations of ultracold gases and in the application of atomic ensembles and single atoms for cavity QED and quantum information studies. Recent progress includes the trapping and control of single atoms in dynamic potentials [1, 2], the sub-micron positioning of individual atoms with standing-wave potentials [3, 4], micro-structured and dynamic traps for Bose–Einstein condensates [5, 6], and, as another example, the realization of chaotic dynamics in atom-optics 'billiards' [7, 8].

The reaction of trapped atoms to dynamical variation of the trapping potential is one central aspect of these developments. Its understanding is important to design optimally the shape of the potential and its temporal variations, which provide the desired control over the atoms and allow their manipulation. The question of efficiently steering atoms by dynamically variable light beams shares many similarities with the application of laser beams for optical tweezers, for manipulating microscopic objects such as beads or living cells [9]. In the context of quantum information processing, it is also related to recent developments towards position control of single trapped ions in complex, multi-segment ion traps [10].

We report on a particular case of manipulation of atoms by dynamic variation of light potentials formed by laser beams: the transfer of a cold cloud of rubidium atoms between two horizontal, intersecting, focused laser beams. The transfer

*Corresponding author. Email: Juergen.Eschner@icfo.es
‡Present address: Cassel Messtechnik GmbH, Dransfeld, Germany.
§Present address: ICFO – Institut de Ciencies Fotoniques, 08860 Castelldefels (Barcelona), Spain.
¶Present address: Institut für Quantenphysik, Universität Ulm, Germany.

Journal of Modern Optics
ISSN 0950–0340 print/ISSN 1362–3044 online © 2007 Taylor & Francis
http://www.tandf.co.uk/journals
DOI: 10.1080/09500340600861740

happens by ramping the intensities in the two beams, which is done slowly enough to give all atoms time to adjust to the change. The measured signal is the amount of atoms remaining in the second beam after the first one has been fully switched off, i.e. the transfer efficiency. Our main finding is a peculiar dependence of the efficiency on the vertical distance between the two beams, which we vary within about ± 3 times the beam waist radius ω_0. The striking result is that we observe optimum transfer when the beams are not fully overlapping but when the distance between their axes is about ω_0. When the beams cross with maximum overlap the transfer efficiency is reduced by about a factor of two.

The observed behaviour is reproduced in numerical simulations of the situation, using classical trajectories of independent atoms. Supported by these results, our explanation is that the finite distance of ω_0 between the beams provides a favourable geometry for scattering an atom from one beam to the other, because it does not create any potential barrier, while at the same time the anharmonicity of the combined potential mixes the degrees of freedom of orthogonal directions.

2. Experiment

In the experiment, we trap a cloud of ^{87}Rb atoms in a dipole trap formed by about 0.7 W of light from a Ti:Sapphire laser at 810.0 nm, focused to a waist diameter of about $2\omega_0 = 15\,\mu$m. The atoms are transferred into the dipole trap from a standard magneto-optical trap (MOT) formed by three retro-reflected beams from a frequency-stabilized diode laser [11]. After switching off the MOT, the atoms are held in the dipole trap for 100 ms, during which they thermalize. Then the second, orthogonal laser beam is ramped up from 0 to to 0.4 W within 100 ms, followed by ramping down the first beam to zero during the next 100 ms. After another 220 ms of waiting time, the MOT beams are switched back on, the dipole trap is switched off completely, and the fluorescence of the recaptured atoms is measured over 100 ms. The procedure is repeated several times to average shot-to-shot fluctuations in the initial number of trapped atoms.

The two dipole trapping beams are horizontal and have the same beam parameters. At their respective maximum powers of 0.7 and 0.4 W, the single-beam potentials are 150 and 86 MHz deep and have 42 and 32 kHz radial frequencies. Ramping them is done with acousto-optical modulators (AOMs), while mechanical shutters are used to switch them off completely before and after ramping. The beams intersect at their focal points, apart from an adjustable vertical distance, which is the main experimental parameter. Vertical adjustment is done by a precision translation stage that moves the complete assembly of fibre collimator and focusing lens which provides the second trapping beam.

The main experimental result is shown in figure 1. On variation of the vertical distance, the transfer efficiency exhibits two maxima, around $\pm\omega_0$. In the symmetric situation, at maximum overlap of the beams, the efficiency is reduced, and, obviously, it goes to zero when the beam distance becomes large.

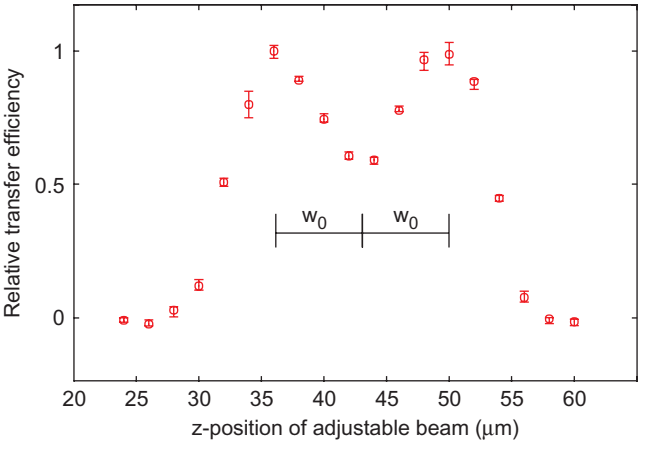

Figure 1. Measured transfer efficiency between the two trapping beams as a function of their vertical distance apart. The error bars correspond to a confidence level of 68%, determined from several 10 repetitions of the same measurement. The efficiency is normalized to the maximum.

3. Qualitative description

The probability of an atom being transferred from one beam to the other depends on the shape of the combined potential in the crossing region and on the kinetic energy of the atom. Here we provide a qualitative discussion of the physical situation, before we present a numerical simulation of the dynamics in the next section.

We denote the three spatial directions by $\hat{x}$ for the propagation direction of the first beam, $\hat{y}$ for that of the second, and $\hat{z}$ for the vertical direction. In figure 2, we show three relevant cases of vertical distance, assuming equal beam power. For zero distance the two beams combine to form one localized 3-dimensional potential 'dimple', which is symmetric in $\hat{x}$ and $\hat{y}$, and stronger in $\hat{z}$. For a distance larger than ω_0, a potential barrier separates the two beams. In the intermediate case of separation by ω_0, neither a dimple nor a barrier is formed. Instead, in the $\hat{z}$ direction the potential has a non-Gaussian, flat-bottom shape.

Some qualitative conclusions can be drawn from these pictures. At zero beam separation and for an atom with small kinetic energy, the trajectory will not be affected significantly when it traverses the beam-crossing region, except for a faster radial oscillation and some longitudinal acceleration and deceleration. The potential is always close to harmonic and symmetric. Due to this symmetry, the motion will remain centred around the axis of the beam in which the atom enters the crossing region, and the three directions of motion are not mixed. Thus a transfer between the beams is not likely.

In the case of large beam separation, the potential barrier impedes the transfer, so the probability that an atom changes between the beams falls off to zero. The fall-off is expected to happen faster (i.e. at smaller beam separation) for atoms with lower energy.

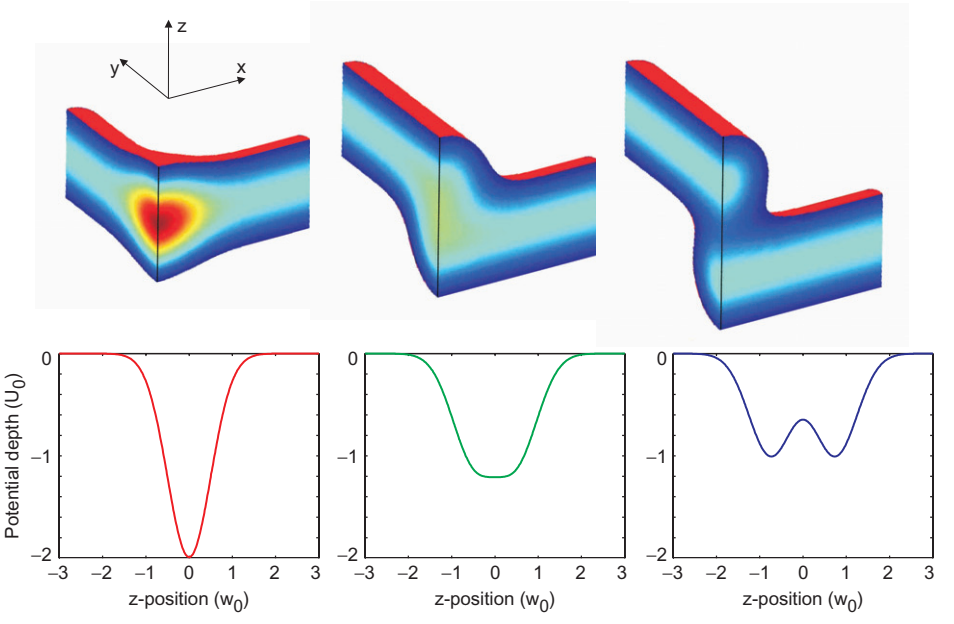

Figure 2. Illustration of the potential in the crossing region, for the vertical distance between the beams set to 0 (left), ω_0 (centre) and $1.5\omega_0$ (right). Top: colour- (or grey-scale-) coded 3-dimensional display. Bottom: vertical potential variation at the centre of the crossing region (along the black line in the top display). (The colour version of this figure is included in the online version of the journal.)

The maximal transfer probability is observed in the intermediate case. We ascribe this to the asymmetric potential in the crossing region, which deflects all incoming atoms upwards or downwards towards the axis of the other beam, such that the motional degrees of freedom become necessarily coupled. Moreover, the potential in the crossing region is anharmonic, which enhances the mixing between the directions.

4. Model calculations

Numerical simulations of the classical motion of a particle in the crossed-beam potential serve as a complementary approach to understand the observed dynamics. Based on the analytical expressions for the potential and its spatial gradient, the differential equations of motion were solved numerically using standard tools [12]. At typical atom temperatures of 50 μK and densities of several $10^{10}\mathrm{cm}^{-3}$, the classical trajectory approach is well justified. Instead of simulating the complete transfer process, which would have required significantly more computational resources, we looked at the dynamics of a single particle in the potential formed by two beams of constant, equal power. Hence these calculations highlight the effect of

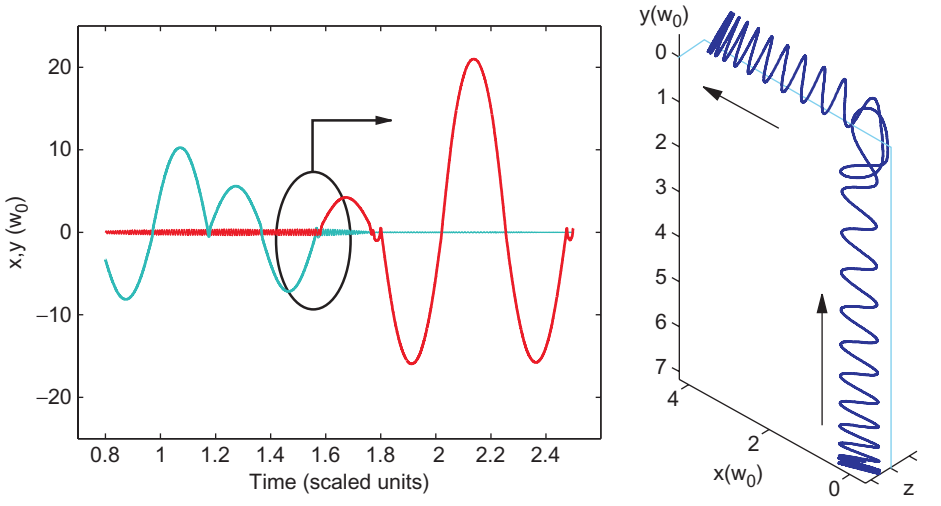

Figure 3. Sample trajectory from the numerical simulation for a beam separation of ω_0. Left: excursion in $\hat{x}$ and $\hat{y}$ in units of ω_0, versus time; $\hat{z}$-motion is not shown. Right: 3-dimensional display zooming into the circled region of the left plot which shows a transfer event. (The colour version of this figure is included in the online version of the journal.)

the coupling between the motional degrees of freedom in the crossing region, and of the potential barrier (when it exists) between the beams.

Figure 3 shows a sample trajectory, for a displacement between the beams equal to the beam waist ω_0. The numerical calculations were programmed with high temporal resolution to account for the strongly different trap frequencies and for the anharmonic potential encountered by particles off the beam axes. In the simulations the total energy (the sum of kinetic and potential energy) was found to change slowly with time, due to accumulated numerical errors, but it was practically constant during a single transit through the crossing region, such that it served as a parameter characterizing each transit event. The probability of a transfer from one beam to the other during a transit through the crossing region was then recorded as a function of the energy and the beam separation. A particle was considered to be transferred between the beams if it entered the crossing region (defined as $\pm 3\omega_0$ around the center) along one beam and exited it along the other. A transit was defined as any event where the particle entered and left the crossing region in either of the beams. The transfer probability is the ratio of the number of transfers to the number of transits. The initial conditions were chosen at random; gravity was neglected [13].

Figure 4 shows a histogram of transfer probability versus beam separation and particle energy from such a numerical investigation. The value of each bin is based on 100 to 1000 transit events.

Its general features agree well with the qualitative explanation given earlier. At small beam separation, significant transfer only happens at high particle energies. At beam separations around ω_0, the transfer probability is more equally spread over all possible energies, and generally much higher than in the case of small beam separation. Beam separations exceeding ω_0 show no transfer at low particle energies,

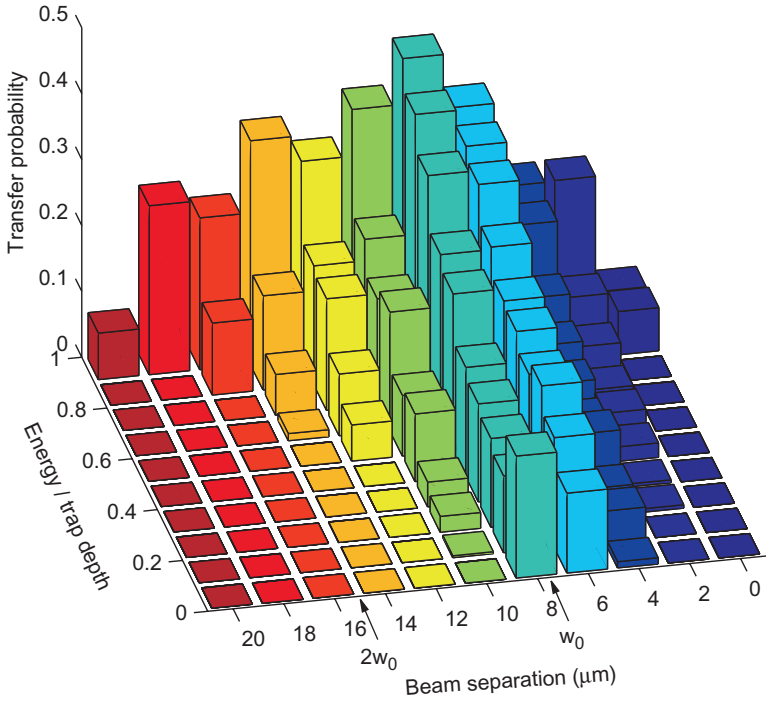

Figure 4. Simulated transfer efficiency versus beam separation, at different values of the total energy of the particle. (The colour version of this figure is included in the online version of the journal.)

due to the potential barrier between the beams; the excluded energy range grows with increasing separation.

Finally, figure 5 shows the simulated transfer probability versus beam separation for a thermal distribution of atoms; this diagram must be compared with the experimental result of figure 1. It was calculated from the data of figure 4 by weighting them with a thermal distribution of particle energy in a 3-dimensional harmonic oscillator. The temperature was taken to be 10% of the trap depth, which we determined in independent measurements, and which has also been consistently found in several other experiments [14].

The simulated transfer probability is maximal around a beam separation of ω_0, with a pronounced minimum at the position of perfect crossing of the beams. For separations larger than ω_0, the probability falls off steeply. Therefore, the main features of the measurement are already well reflected in these simple simulations, using a static trap potential of Gaussian beams. The largest deviation between experiment and simulation is observed for small beam separation, where the measured transfer probability is significantly higher. We attribute this to the transient situation of non-equal intensities of the beams during ramp-up and ramp-down in the experiment, which is less symmetric and may therefore mix the motion more efficiently. Other effects, such as elastic collisions between atoms in the crossing

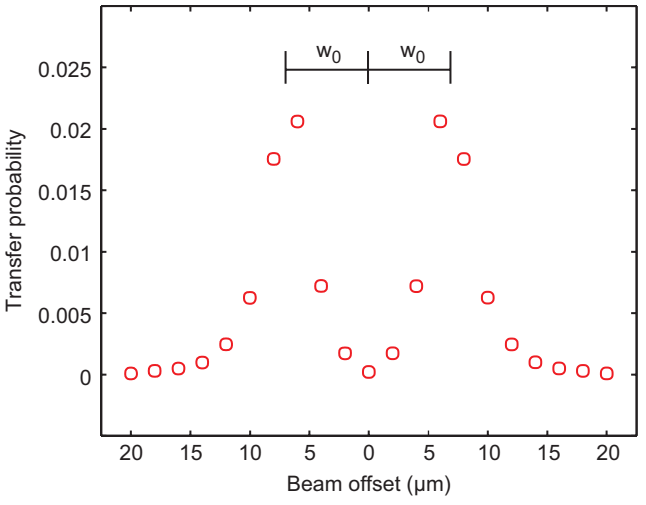

Figure 5. Simulated transfer efficiency versus beam separation, for a thermal distribution of particle energies as in the experiment. This diagram must be compared to figure 1.

region, may also play a role in redistributing energy among the three modes of oscillation, and thus enhance the transfer efficiency at small beam separation for a cloud of atoms, as in the experiment, relative to the simulated single-particle case. We exclude, on the other hand, that experimental inaccuracies, such as non-Gaussian beam shapes or beam pointing instabilities, have broadened the central part of the measured efficiency curve, because no such broadening is observed on the outer wings of the curve.

5. Conclusions

In summary, we have measured the transfer of trapped atoms between two crossed laser beams, varying the distance between the beams. We find optimum transfer at non-zero beam separation, when the mixing between the motional degrees of freedom is favoured by the anharmonic potential, while no potential barrier is formed between the beams. The main characteristics of the experimental observations are reproduced in numerical simulations of the dynamics. They become visible already in the situation of two crossed beams of constant, equal power. Our results are relevant for designing efficient loading mechanisms for optical traps and optical lattices, and they may find applications in optical tweezer technology for nano- and micro-particles.

Acknowledgments

This work was supported in part by the Austrian Science Fund (FWF, Project SFB15) and by the European Commission (QGATES, IST-2001-38875).

References

[1] S. Bergamini, B. Darqui, M. Jones, *et al.*, J. Opt. Soc. Am. B **21** 1889 (2004); J. Beugnon, M.P.A. Jones, J. Dingjan, *et al.*, Nature **440** 779 (2006).
[2] D.D. Yavuz, P.B. Kulatunga, E. Urban, *et al.*, Phys. Rev. Lett **96** 063001 (2006).
[3] D. Schrader, I. Dotsenko, M. Khudaverdyan, *et al.*, Phys. Rev. Lett. **93** 150501 (2004); I. Dotsenko, W. Alt, M. Khudaverdyan, *et al.*, Phys. Rev. Lett. **95** 033002 (2005).
[4] J.A. Sauer, K.M. Fortier, M.S. Chang, *et al.*, Phys. Rev. A **69** 051804(R) (2004).
[5] T.P. Meyrath, F. Schreck, J.L. Hanssen, *et al.*, Phys. Rev. A **71** 041604(R) (2005).
[6] V. Boyer, R.M. Godun, G. Smirne, *et al.*, Phys. Rev. A **73** 031402(R) (2006).
[7] V. Milner, J.L. Hanssen, W.C. Campbell and M.G. Raizen, Phys. Rev. Lett. **86** 1514 (2001).
[8] N. Friedman, A. Kaplan, D. Carasso and N. Davidson, Phys. Rev. Lett. **86** 1518 (2001).
[9] A. Ashkin, J.M. Dziedzic, J.E. Bjorkholm and S. Chu, Opt. Lett. **11** 288 (1986); A. Ashkin, Proc. Natl. Acad. Sci. USA **94** 4853 (1997); K. Dholakia, G. Spalding and M. MacDonald, Physics World 15, **31** (2002); K.C. Neuman and S.M. Block, Rev. Sci. Instr. **75** 2787 (2004).
[10] W.K. Hensinger, S. Olmschenk, D. Stick, *et al.*, Appl. Phys. Lett. **88** 034101 (2006).
[11] More details of the experimental apparatus can be found in: M. Schulz, PhD thesis, Innsbruck 2003. See http://heart-c704.uibk.ac.at
[12] We used the ODE45 routine in MATLAB.
[13] The optical potentials within the focus region of about 10 μm size are at a level of tens of MHz, such that gravity (~2.5 kHz/μm) can be ignored for a principal understanding of the dynamics.
[14] K.M. O'Hara, M.E. Gehm, S.R. Granade and J.E. Thomas, Phys. Rev. A **64** 051403(R) (2001).